Journal of Agrometeorology
(A publication of Association of Agrometeorologists)
ISSN : 0972-1665 (print), 2583-2980 (online)
Vol. No. 28 (3) : 336-344 (September - 2026)
https://doi.org/10.54386/jam.v28i3.3405
https://journal.agrimetassociation.org/index.php/jam

Research paper

Application of MCDM Techniques in Ranking of CMIP6 GCMs for Extreme Temperatures over the Periyar River Basin

MARK ARNOLD BULSARI, GANESH D. KALE* and JARPALA VENKATESH

Department of Civil Engineering, Sardar Vallabhbhai National Institute of Technology, Surat, Gujarat, India
**Corresponding author email: gdk@ced.svnit.ac.in*

ABSTRACT

Climatic extremes like temperature extremes are susceptible to climate change (CLC) warming impacts. Thus, it is essential to study the effect of CLC on extreme temperatures (minimum temperature, *i.e.,* T_{min} and maximum temperature, *i.e.,* T_{max}) of the Periyar River Basin (PRB), which has several human-induced constraints. Choosing the best general circulation models (GCMs) from a set through ranking is needed for precise projections of future climatic variables. None of the reviewed studies has executed GCMs ranking for 6th phase of Coupled Model Intercomparison Project (CMIP6) corresponding to extreme temperatures of the PRB. Thus, in the current study, ranking of 27 CMIP6 GCMs is performed for extreme temperatures at every grid point of the PRB by using four performance indicators, entropy method and Compromise Programming (CP) and Technique for Order Preference by Similarity to an Ideal Solution (TOPSIS). The aggregated ranking of GCMs corresponding to the whole study area for extreme temperatures is also executed by employing the Group Decision-Making Approach (GDMA). Top six ranked GCMs obtained through GDMA for T_{max} are FGOALS-g3, BCC-CSM2-MR, CanESM5, GFDL-CM4-gr2, GISS-E2-1- G and CNRM-CM6-1 corresponding to TOPSIS and CP techniques while that for T_{min} are KIOST-ESM, CanESM5, CNRM-CM6-1, INM-CM5-0, INM- CM4-8 and GISS-E2-1-G.

Keywords: Extreme Temperatures; Periyar River Basin; Ranking; TOPSIS; Compromise Programming; GDMA

Climate Change (CLC) is contemplated to be the most severe environmental issue the modern world has ever faced (Salman *et al.,* 2018). According to the Intergovernmental Panel on CLC's Fifth Assessment Report (IPCC AR5), global temperatures have been increasing since 1880 and are projected to rise continuously (Jia *et al.,* 2019). General circulation models (GCMs) are the primary tools used in CLC studies for projecting future CLC, which is needed in the assessment of CLC effect on water resources and hydrology (Zamani & Berndtsson, 2019). These models accurately estimate or replicate present and future values for numerous climatic parameters (Srinivasa Raju & Nagesh Kumar, 2015).

The World Climate Research Program was invigorated for the creation of the Coupled Model Intercomparison Project (CMIP) (Sun *et al.,* 2015). CMIP includes modelling of past, current and future climatic conditions (Seker & Gumus, 2022). Numerous GCMs have been developed over the years and the CMIP's structure has evolved from its original version, *i.e.,* CMIP1, to the recently designed version CMIP6 (Salehie *et al.,* 2023). The main dissimilarities amongst the CMIP6 simulations and preceding CMIP phases such as CMIP3 and CMIP5 are the beginning years of future scenarios and different sets of specifications corresponding to concentration, emissions and land-use scenarios (Shiru & Chung, 2021). However, significant uncertainties are linked with the climate simulated by GCMs because of factors like model structure, parameterization, assumptions, calibration methodologies and others (Khan *et al.,* 2018). One way of reducing uncertainty associated with GCMs is ranking of GCMs.

To rank GCMs from various collections, it is necessary to explore multiple multi-criteria decision-making (MCDM) techniques and performance indicators (PIs) across different categories at the watershed level (Jose & Dwarakish, 2022). The Technique for Order Preference by Similarity to an Ideal Solution,

Article info - DOI: *https://doi.org/10.54386/jam.v28i3.3405*
Received:03 March 2026; Accepted: 14 July 2026; Published online : 7 September 2026

i.e., TOPSIS operates on the norm that the preferred alternative should have the greatest distance from the non-ideal solution and the minimal distance from the ideal solution (Srinivasa Raju & Nagesh Kumar, 2015). Compromise programming (CP) is a popular MCDM approach applied in a variety of arenas, including climate research. Its main principle is to determine an ideal point at which each studied characteristic achieves its best value (Shiru & Chung, 2021).

The Western Ghats region has around 45 rivers including the Periyar River (PR), which is one of the South India's major rivers (Sadhwani *et al.,* 2023). The PR Basin (PRB) is a humid tropical watershed located in the Western Ghats. It is a complex watershed characterized by various man-made constraints (Sadhwani & Eldho, 2023). Climatic extremes like temperature extremes are susceptible to the effects of CLC warming, and these extremes are often associated with significant consequences for ecosystems (Lei *et al.,* 2023). Therefore, it is necessary to assess the influence of CLC on future extreme temperatures in the PRB for which the use of credible CMIP6 GCMs is crucial. Therefore, ranking of GCMs is needed to determine best GCMs for simulating future extreme temperatures of the PRB. Therefore, a literature review is performed on the ranking of GCMs for river basins corresponding to temperature extremes. Several researchers have performed a ranking of GCMs for river basins for extreme temperatures (Loganathan & Mahindrakar, 2020; Pradhan *et al.,* 2021; Jose & Dwarakish, 2022; Gebisa *et al.,* 2023; Lebeza *et al.,* 2024 etc). From the reviewed literature, the following research gaps are inferred: 1) none of the reviewed studies have performed a ranking of CMIP6 GCMs for maximum temperature (T_{max}) and minimum temperature (T_{min}) variables of the PRB and 2) none of the reviewed studies have used 27 CMIP6 GCMs for the ranking. Aforesaid research gaps are addressed in the present study by performing a ranking of twenty-seven NEX-GDDP CMIP6 GCMs for T_{max} and T_{min} variables of the PRB. In the present study, spatially explicit and multi-criteria framework which includes weighing of PIs is used which is better as compared to simple approaches.

MATERIALS AND METHODS

Study Area

With a length of around 244 kilometres, the PR is Kerala's 2nd longest river. The river flows from the Sivagiri hill, which is located 80 kilometres south of the Devikulam district in India's Western Ghats and is 2438 meters above the mean sea level. It flows westward towards the Arabian Sea, featuring the highest peak within the basin *i.e.*, Anamudi Peak. The PRB is extended over the longitudes 76° to 77° 30′ East and latitudes 9° 16′ to 10° 20′ North. On an average, the basin experiences a yearly rainfall of 3200 mm. As a perennial river, the PR is a crucial water source for the central area of the Kerala state. The T_{max} in the basin typically varies from 25 to 32 degrees Celsius, while the T_{min} varies between 14 and 19 degrees Celsius (Sadhwani *et al.,* 2023). Fig. 1 shows index map of the PRB.

Data Collection

Extreme temperatures data derived from GCMs

The NASA Earth Exchange Global Daily Downscaled Projections (NEX-GDDP) were initially introduced in 2015 in the form of NEX-GDDP-CMIP5 and since then these have become a valuable resource for assessing the global and local impacts of CLC. The recent form of NEX- GDDP data (particularly NEX-GDDP-CMIP6) incorporates downscaled data from 35 models covering the period of 1950-2100. It includes both historical records and future projections based on CMIP6 findings. The NEX-GDDP-CMIP6 datasets employ spatial disaggregation and bias correction techniques to consistently downscale the original CMIP6 outputs to provide daily data at a spatial resolution of 0.25° × 0.25° (Zhang *et al.,* 2023).

The data of T_{max} and T_{min} corresponding to 27 GCMs of NEX-GDDP CMIP6 datasets are downloaded from a website (https://www.nccs.nasa.gov/services/data-collections/land-based-products/nex-gddp-cmip6). In this study, 27 GCMs' T_{max} and T_{min} data corresponding to historical period (1970-2014) are used.

Observed extreme temperature data

The Climate Research Unit (CRU) gridded time series is a prominent climatic dataset known for its global coverage, excluding Antarctica, with a grid resolution of 0.5° x 0.5°. This dataset was meticulously created by interpolating monthly climatic anomalies from widespread networks of weather station observations (Harris *et al.,* 2020). CRU data of extreme temperatures was available from year 1970. Thus, in the present study, CRU data of extreme temperatures over the period of 1970 to 2014 are used. The bilinear interpolation approach is used to re-grid the CRU data to a resolution of 0.25° × 0.25°. In this study, CRU gridded T_{max} and T_{min} data corresponding to the period 1970 to 2014 are used as reference data for the baseline period.

Methodology

For T_{max} and T_{min} variables, GCMs are ranked separately at each grid point by using PIs such as Kling-Gupta Efficiency (KGE) (Ahmed *et al.,* 2019), Normalized Root Mean Square Error (NRMSE) (Zamani & Berndtsson, 2019), Nash-Sutcliffe Efficiency (NSE) (Hassan *et al.,* 2020) and Correlation Coefficient (CC) (Srinivasa Raju *et al.,* 2017). Both simulated data (GCMs data) and observed data (CRU data) at 21 grid points over the PRB corresponding to T_{max} and T_{min} variables are used to calculate aforementioned PIs at each grid point for the period 1970-2014. Following that, PIs are normalized and weights are allocated to each PI by employing Entropy technique (Sreelatha & AnandRaj, 2020) for every GCM at each grid point and then the best GCMs are selected by using two MCDM approaches at each grid point. The entropy weight for each PI is calculated from its normalized value, with the final weight being proportional to the degree of diversification, such that indicator with higher information content is assigned greater weight. The MCDM techniques used in the present

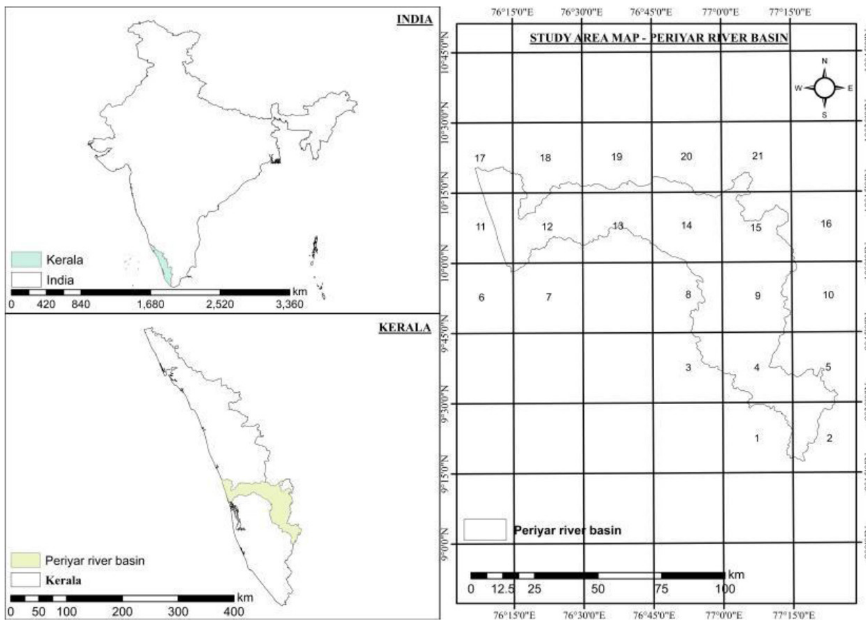

Fig. 1: Index map of the PRB

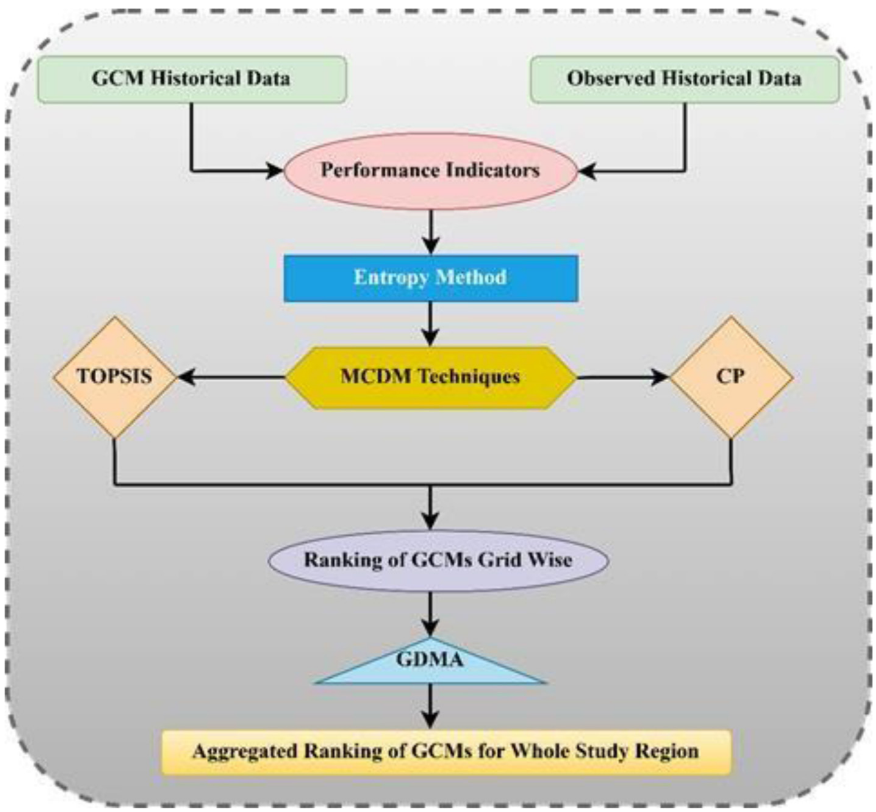

Fig. 2: Methodology flowchart

study are TOPSIS (Zamani & Berndtsson, 2019; Venkatesh & Kale, 2025) and CP (Srinivasa Raju *et al.,* 2017). While several established MCDM frameworks exist, TOPSIS and CP are specifically selected to formulate a robust, dual-method evaluation framework that minimizes parameter subjectivity. Next, the Group Decision-Making Approach, *i.e.*, GDMA (Sreelatha & AnandRaj, 2020) is used to aggregate ranks of GCMs for the entire study area corresponding to two MCDM techniques. When grid points are intended, GDMA is

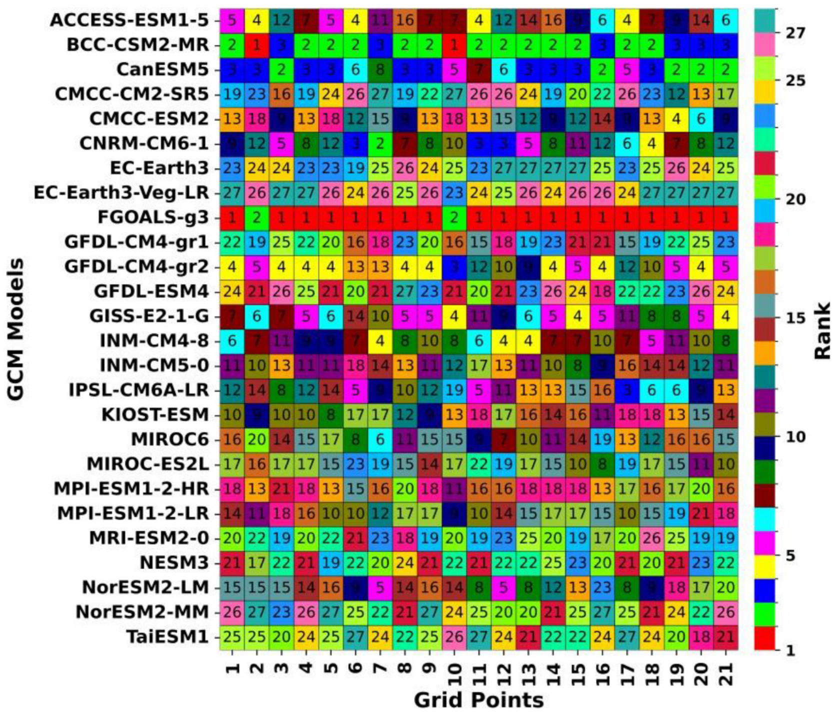

Fig. 3: Grid wise ranking of GCMs for T_{max} over the PRB by using CP technique

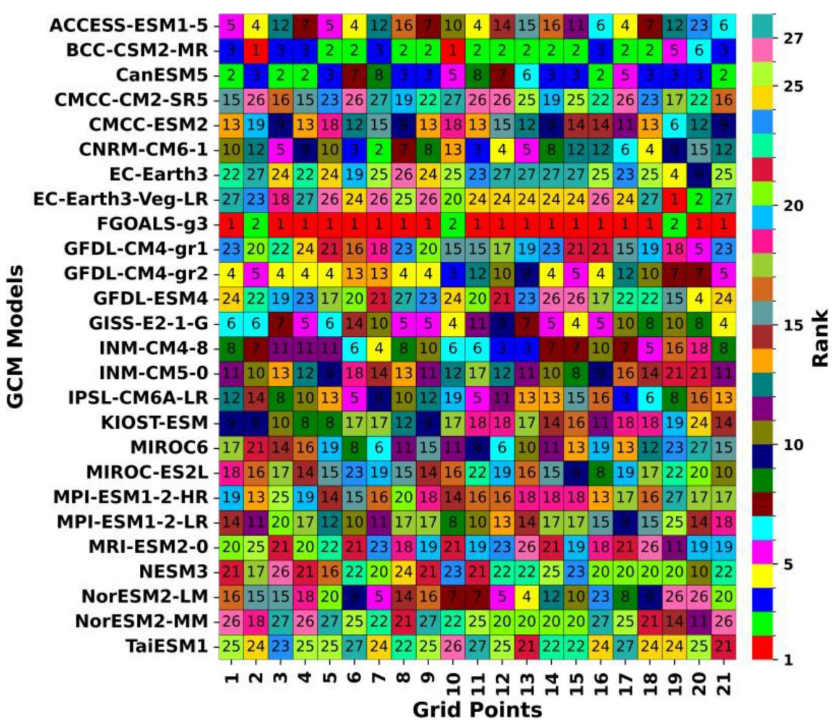

Fig. 4: Grid wise ranking of GCMs for T_{max} over the PRB by using TOPSIS technique

the process used for inferring the best option. Rankings are arranged in the descending manner and these are divided into two parts viz. upper and lower parts. Net strength of the each GCM model is calculated based on strength and weakness of the model. The GCM with highest net strength is given preference while other GCMs are ranked accordingly in descending manner (Sreelatha & AnandRaj, 2020). Methodology used in the present study is shown in the flow chart below (Fig. 2).

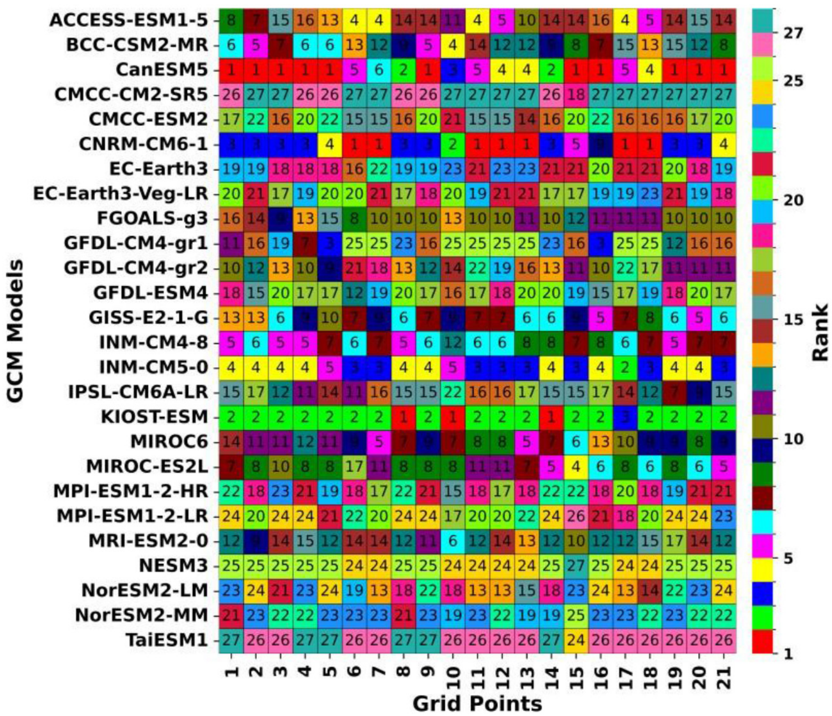

Fig. 5: Grid wise ranking of GCMs for T_{min} over the PRB by using CP technique

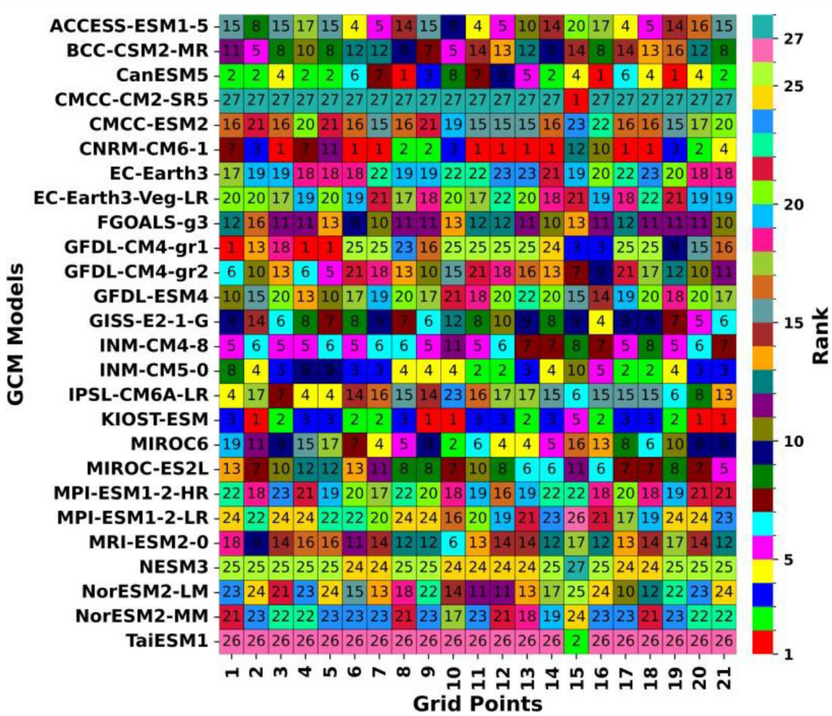

Fig. 6: Grid wise ranking of GCMs for T_{min} over the PRB by using TOPSIS technique

RESULTS AND DISCUSSION

Ranking of CMIP6 GCMS by Using TOPSIS and CP Methods

For T_{max} and T_{min} variables, the values of CC, NRMSE, NSE, and KGE are estimated corresponding to monthly scale for every GCM at each grid point for the baseline period of 1970- 2014. Here results of ranking of GCMs at grid point 8 (9.875 N * 76.875 E, latitude and longitude) are presented as an illustration. For CC, KGE and NSE, the ideal value is 1 whereas that for NRMSE it is 0. The weights assigned to the PIs at grid point 8 are as follows: for T_{max},

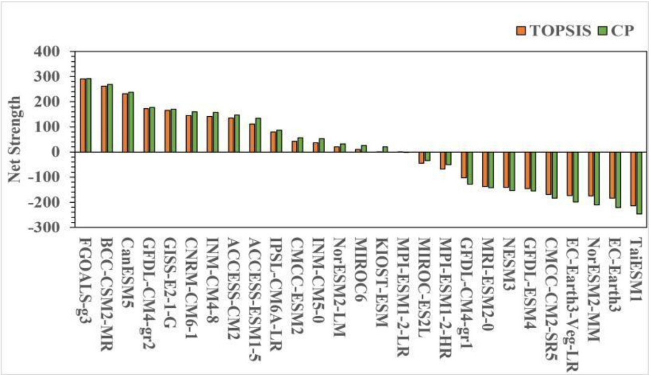

Fig. 7: Net strength of 27 NEX-GDDP CMIP6 GCMs based on GDMA corresponding to TOPSIS and CP methods for T_{max} variable, respectively.

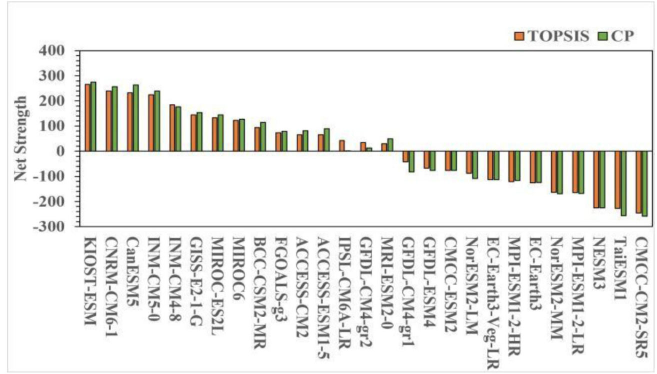

Fig. 8: Net strength of 27 NEX-GDDP CMIP6 GCMs based on GDMA corresponding to TOPSIS and CP methods for T_{min} variable, respectively.

CC (3%), NRMSE (16%), NSE (75%), and KGE (6%) whereas for T_{min}, CC (2%), NRMSE (62%), NSE (33%), and KGE (3%).

For T_{max}, FGOALS-g3 GCM and GFDL-ESM4 GCM are found to be the best and worst performing GCMs corresponding to TOPSIS and CP techniques at grid point 8. In case of T_{min}, CanESM5 and KIOST-ESM GCMs are found to be the best performing GCMs whereas CMCC- ESM2 and TaiESM1 GCMs are found to be the worst performing GCMs corresponding to TOPSIS and CP techniques at grid point 8. Similar process is followed for the ranking of GCMs at remaining grid points by using TOPSIS and CP methods corresponding to T_{max} and T_{min} variables. It is also observed that, the ranking pattern observed for T_{max} is same for both TOPSIS and CP techniques while that for T_{min} it is slightly different.

Spatial Ranking of GCMs Across Grid Points

The spatial (grid wise) ranking results for the 27 GCMs across 21 grid points are presented in the form of heatmaps in Figs. 3-6 by using TOPSIS and CP techniques for T_{max} and T_{min} variables, respectively. The heatmaps indicate that, model performance is not spatially uniform throughout the PRB region. For T_{max}, FGOALS-g3, BCC-CSM2-MR, and CanESM5 consistently achieved the highest ranks across most of the grid points under both TOPSIS and CP methods, demonstrating their strong capability to represent T_{max} conditions within the PRB area. In contrast, several models exhibited substantial fluctuations in ranking, suggesting location-dependent performance characteristics.

Similarly, the T_{min} ranking results revealed that, KIOST-ESM, CanESM5, and INM-CM5-0 are the most consistently high-performing models across the majority of grid points. The persistence of these models among the top-ranked positions indicates their robustness in simulating T_{min} variability across the study area. Although minor differences in rankings were observed among individual grid points, the overall ranking patterns remained largely consistent.

A comparison between the TOPSIS and CP ranking approaches showed strong agreement in identifying the best-performing GCMs for both T_{max} and T_{min}. The consistency of the top-ranked models across the two independent MCDM techniques enhances confidence in the reliability of the model selection process. Therefore, the identified top-performing GCMs may be considered suitable for subsequent climate change impact assessments and future climate projection analyses in the PRB region.

***Aggregated Ranks of GCMs for T_{max} and T_{min} Based on GDMA for Entire Study Area* Corresponding to TOPSIS and CP Methods**

The ranking pattern noticed at various grid points are different. Therefore, to aggregate ranking pattern over the whole study area by using ranking patterns obtained at 21 grid points, the GDMA method is used. Figs. 7 and 8 shows the aggregated ranks of GCMs based on GDMA corresponding to TOPSIS and CP techniques for T_{max} and T_{min} variables. For T_{max}, FGOALS-g3 GCM is found to be the top ranked GCM with net strengths of 291 and 292 by using TOPSIS and CP methods, respectively. On the other hand, TaiESM1 GCMs is found to be the last ranked GCMs with net strengths of -214 and -246 by using TOPSIS and CP techniques, respectively for T_{max} as shown in Fig. 5.

For T_{min}, KIOST-ESM GCM is found to be the top ranked GCM with net strengths of 266 and 275 by using TOPSIS and CP methods, respectively. On the other hand, CMCC-CM2-SR5 GCM is found to be the last ranked GCM with net strengths of -246 and -268 by using TOPSIS and CP techniques, respectively for T_{min} as shown in Fig. 8. The aggregated ranking pattern is almost same corresponding to TOPSIS and CP techniques for T_{max} and T_{min} variables.

The average PI over entire PRB demonstrate that, the selected GCMs reproduce both observed T_{max} and T_{min} over the PRB with satisfactory to very good skill. For T_{max}, the CC ranged from 0.81 to 0.85, indicating a strong agreement between observed and simulated temperatures, while NSE values varied between 0.57 and 0.67, reflecting acceptable predictive capability. The KGE values (0.81-0.85) further confirm the robustness of the simulations in capturing the combined effects of correlation, bias, and variability. Similarly, T_{min} simulations exhibited superior performance, with CC values of 0.81-0.86, lower NRMSE values (0.53-0.60), higher NSE values (0.64-0.72) and consistently high

Table 1: PI values of top 5 ranked GCMs for T_{max} and T_{min} for the entire PRB basin

GCM Name	T_{max}				GCM Name	T_{min}			
	CC	NRMSE	NSE	KGE		CC	NRMSE	NSE	KGE
FGOALS-g3	0.85	0.58	0.67	0.85	KIOST-ESM	0.86	0.53	0.72	0.85
BCC-CSM2-MR	0.84	0.61	0.63	0.84	CNRM-CM6-1	0.85	0.54	0.70	0.84
CanESM5	0.83	0.61	0.62	0.83	CanESM5	0.86	0.53	0.72	0.85
GFDL-CM4-gr2	0.82	0.64	0.58	0.82	INM-CM5-0	0.83	0.57	0.67	0.82
GISS-E2-1-G	0.81	0.65	0.57	0.81	INM-CM4-8	0.81	0.60	0.64	0.80

KGE values (0.80-0.85). Overall, the evaluated GCMs show adequate skill for representing the T_{max} and T_{min} over the PRB, thereby supporting their applicability for future climate impact assessments and adaptation studies in the basin. PI values of top 5 ranked GCMs for T_{max} and T_{min} variables are shown in Table 1.

Sensitivity Analysis of GDMA-Based GCM Rankings

A sensitivity analysis is performed to evaluate the robustness of the final GDMA rankings derived from the TOPSIS and CP methods. The original scenario (S1), which incorporated all four PIs (CC, NRMSE, NSE, and KGE) is compared with four alternative scenarios: S2 (without CC), S3 (without KGE), S4 (without NRMSE), and S5 (without NSE). Spearman rank correlation coefficients are computed between the rankings obtained from S1 and those generated under the alternative scenarios (S2-S5).

For T_{max}, the CP-based rankings exhibited exceptionally high correlations of S2 to S5 scenarios with the original scenario, ranging from 0.9969 to 0.9998. The highest correlation is observed between S1 and S4 scenarios (ρ = 0.9998), indicating that the exclusion of NRMSE has a negligible impact on the final rankings. Similarly, strong correlations are obtained between S1 and S2 (ρ = 0.9982), S1 and S3 (ρ = 0.9976), and S1 and S5 (ρ = 0.9969), demonstrating the stability of the CP ranking framework. The TOPSIS-based T_{max} rankings of S2 to S5 scenarios have also showed strong agreement with the original scenario, with correlation coefficients ranging from 0.9886 to 0.9942. Among the evaluated indicators, the exclusion of KGE (S3) produced the largest ranking variation, although the correlation remained very high (ρ = 0.9886).

For T_{min}, the CP method yielded correlation coefficients between S1 and S2 to S5 scenarios in the range of 0.9834 and 0.9992. The highest agreement is observed between S1 and S4 (ρ = 0.9992), while the lowest correlation is observed between S1 and S5 (ρ = 0.9834), suggesting that, NSE had a relatively greater influence on T_{min} rankings as compared to the other indicators. Similarly, the TOPSIS method produced strong correlations ranging from 0.9774 to 0.9976. The lowest correlation is again observed when NSE is excluded (for S1 and S5; ρ = 0.9774), indicating that NSE contributed more to the T_{min} ranking structure than the remaining performance measures.

Overall, the consistently high Spearman correlation coefficients obtained for both T_{max} and T_{min} demonstrate that the GDMA-based rankings are robust and insensitive to the exclusion of any single PI. The persistence of ranking patterns across all sensitivity scenarios confirms the reliability of the entropy-weighted TOPSIS and CP frameworks and strengthens confidence in the final GCM selection for the PRB. Nevertheless, the slightly lower correlations associated with the exclusion of NSE, particularly for T_{min}, suggest that this indicator plays a comparatively more influential role in determining model rankings.

CONCLUSION

In the present study, ranking of 27 CMIP6 GCMs is performed for extreme temperatures at every grid point of the PRB by using four PIs, entropy method and TOPSIS and CP MCDM techniques followed by aggregated ranking of GCMs for the whole study area by employing the GDMA. Following conclusions are derived from the present study.

- Dual MCDM framework includes weighing of PIs which is better as compared to simple approaches.
- Application of GDMA corresponding to TOPSIS and CP techniques revealed that, FGOALS-g3, BCC-CSM2-MR and CanESM5 are the common top three aggregated ranked GCMs for T_{max} variable of the PRB.
- Application of the GDMA corresponding to TOPSIS technique revealed that, KIOST- ESM, CNRM-CM6-1 and CanESM5 are the top three aggregated ranked GCMs for T_{min} variable of the PRB.
- Application of the GDMA corresponding to CP technique revealed that, KIOST-ESM, CanESM5 and CNRM-CM6-1 are the top three aggregated ranked GCMs for T_{min} variable of the PRB.
- The sensitivity analysis further confirmed the robustness of the proposed ranking framework, as the GDMA-based rankings obtained by using both TOPSIS and CP remained highly consistent across all sensitivity scenarios, with Spearman correlation coefficients exceeding 0.97.
- Top performing GCMs selected in the present study for extreme temperatures can be used for ensemble construction corresponding to future climate assessments and future projections of hydroclimatic variables of the PRB.
- This enhanced performance of top selected GCMs may be associated with improvements in the representation of key climatic processes used in the respective models, including atmospheric dynamics, land-surface interactions, and coupled Earth-system processes. Similar skill as that of several top

ranked models identified in the present study has also been reported in neighbouring regions. However, specific physical mechanisms responsible for enhanced performance of top ranked models are not explicitly investigated.

- Despite the robustness of the proposed framework, some limitations should be acknowledged. The entropy weighting method is entirely data-driven and it may assign greater weightage to PIs exhibiting higher variability, potentially approximating a single- criterion dominance under certain conditions. The GDMA is employed to derive an aggregated ranking over the PRB but its performance in this specific application is not validated against an independent benchmark or alternative aggregation framework. The re-gridding of CRU extreme temperatures dataset to NEX-GDDP-CMIP6 outputs to the CRU spatial resolution introduces interpolation-related uncertainties that may affect local-scale estimates of model and, consequently the final rankings.

ACKNOWLEDGMENT

The authors are thankful to Climate Research Unit, UK and NASA Centre for Climate Simulation, USA, for providing necessary data through their portal, which is used in the present study.

Author's certificate: The manuscript or its part is not under consideration for publication elsewhere and the same has been approved by all co-authors.

Conflict of Interests: The authors declare that there is no conflict of interest regarding the publication of this article.

Funding: No funding was received to assist with the preparation of this research.

Data Availability: Data is available freely on the relevant websites.

Author's contribution: **Mark Arnold Bulsari:** Data collection, Analysis, Manuscript writing**; Ganesh D. Kale:** Conceptualization, Supervision, Editing; **Jarpala Venkatesh:** Help in analysis and editing.

Publisher's Note: The periodical remains neutral concerning jurisdictional claims in published maps and institutional affiliations.

Publisher's Note: The periodical remains neutral concerning jurisdictional claims in published maps and institutional affiliations.

REFERENCES

Ahmed, K., Sachindra, D. A., Shahid, S., Demirel, M. C., & Chung, E. S. (2019). Selection of multi-model ensemble of general circulation models for the simulation of precipitation and maximum and minimum temperature based on spatial assessment metrics. *Hydrology and Earth System Sciences*, *23*(11), 4803–4824. https://doi.org/10.5194/hess-23-4803-2019

Gebisa, B. T., Dibaba, W. T., & Kabeta, A. (2023). Evaluation of historical CMIP6 model simulations and future climate change projections in the Baro River Basin. *Journal of Water and Climate Change*, *14*(8), 2680–2705. https://doi.org/10.2166/wcc.2023.032

Harris, I., Osborn, T. J., Jones, P., & Lister, D. (2020). Version 4 of the CRU TS monthly high- resolution gridded multivariate climate dataset. *Scientific Data*, *7*(1), 109. https://doi.org/10.1038/s41597-020-0453-3

Hassan, I., Kalin, R. M., White, C. J., & Aladejana, J. A. (2020). Selection of CMIP5 GCM ensemble for the projection of spatio-temporal changes in precipitation and temperature over the Niger Delta, Nigeria. *Water*, *12*(2), 385. https://doi.org/10.3390/w12020385

Jia, K., Ruan, Y., Yang, Y., & You, Z. (2019). Assessment of CMIP5 GCM simulation performance for temperature projection in the Tibetan Plateau. *Earth and Space Science*, *6*(12), 2362–2378. https://doi.org/10.1029/2019EA000962

Jose, D. M., & Dwarakish, G. S. (2022). Ranking of downscaled CMIP5 and CMIP6 GCMs at a basin scale: Case study of a tropical river basin on the southwest coast of India. *Arabian Journal of Geosciences*, *15*(1), 120. https://doi.org/10.1007/s12517-021-09289-0

Khan, N., Shahid, S., Ahmed, K., Ismail, T., Nawaz, N., & Son, M. (2018). Performance assessment of general circulation model in simulating daily precipitation and temperature using multiple gridded datasets. *Water*, *10*(12), 1793. https://doi.org/10.3390/w10121793

Lei, Y., Peng, P., & Jiang, W. (2023). Evaluation of global climate models for the simulation of precipitation and maximum and minimum temperatures at coarser and finer resolutions based on temporal and spatial assessment metrics in mainland China. *Journal of Water and Climate Change*, *14*(5), 1585–1599. https://doi.org/10.2166/wcc.2023.464

Lebeza, T. M., Gashaw, T., Bayabil, H. K., Van Oel, P. R., Worqlul, A. W., Dile, Y. T., & Chukalla, A. D. (2024). Performance of specific CMIP6 GCMs for simulating the historical rainfall and temperature climatology of Lake Tana sub-basin, Ethiopia. *Scientific African*, *26*, e02387. https://doi.org/10.1016/j.sciaf.2024.e02387

Loganathan, P., & Mahindrakar, A. B. (2020). Assessment and ranking of CMIP5 GCMs performance based on observed statistics over Cauvery River basin–Peninsular India. *Arabian Journal of Geosciences*, 13, 1–11. https://doi.org/10.1007/s12517-020-06217-6

Pradhan, P., Shrestha, S., Sundaram, S. M., & Virdis, S. G. (2021). Evaluation of CMIP5 general circulation models for simulating the precipitation and temperature of the Koshi

River Basin in Nepal. *Journal of Water and Climate Change*, *12*(7), 3282–3296. https://doi.org/10.2166/wcc.2021.124

Sadhwani, K., & Eldho, T. I. (2023). Assessing the vulnerability of water balance to climate change at river basin scale in humid tropics: Implications for a sustainable water future. *Sustainability*, *15*(11), 9135. https://doi.org/10.3390/su15119135

Sadhwani, K., Eldho, T. I., & Karmakar, S. (2023). Investigating the influence of future land use and climate change on hydrological regime of a humid tropical river basin. *Environmental Earth Sciences*, *82*(9), 210. https://doi.org/10.1007/s12665-023-10891-6

Salehie, O., Hamed, M. M., Ismail, T. B., Tam, T. H., & Shahid, S. (2023). Selection of CMIP6 GCM with projection of climate over the Amu Darya River Basin. *Theoretical and Applied Climatology*, *151*(3–4), 1185–1203. https://doi.org/10.1007/s00704-022-04332-w

Salman, S. A., Shahid, S., Ismail, T., Ahmed, K., & Wang, X. J. (2018). Selection of climate models for projection of spatiotemporal changes in temperature of Iraq with uncertainties. *Atmospheric Research*, *213,* 509–522. https://doi.org/10.1016/j.atmosres.2018.07.008

Seker, M., & Gumus, V. (2022). Projection of temperature and precipitation in the Mediterranean region through multi-model ensemble from CMIP6. *Atmospheric Research*, *280*, 106440. https://doi.org/10.1016/j.atmosres.2022.106440

Shiru, M. S., & Chung, E. S. (2021). Performance evaluation of CMIP6 global climate models for selecting models for climate projection over Nigeria. *Theoretical and Applied Climatology*, *146*(1–2), 599–615. https://doi.org/10.1007/s00704-021-03746-2

Sreelatha, K., & AnandRaj, P. (2020). Regional evaluation of global climate models for precipitation, maximum and minimum temperature over southern-part of India. *ISH Journal of Hydraulic Engineering*, *28*(sup1), 449–462. https://doi.org/10.1080/09715010.2020.1779137

Srinivasa Raju, K., & Nagesh Kumar, D. (2015). Ranking general circulation models for India using TOPSIS. *Journal of Water and Climate Change*, *6*(2), 288–299. https://doi.org/10.2166/wcc.2014.074

Srinivasa Raju, K., Sonali, P., & Nagesh Kumar, D. (2017). Ranking of CMIP5-based global climate models for India using compromise programming. *Theoretical and Applied Climatology*, *128*, 563–574. https://doi.org/10.1007/s00704-015-1721-6

Sun, Q., Miao, C., & Duan, Q. (2015). Comparative analysis of CMIP3 and CMIP5 global climate models for simulating the daily mean, maximum, and minimum temperatures and daily precipitation over China. *Journal of Geophysical Research: Atmospheres*, *120*(10), 4806– 4824. https://doi.org/10.1002/2014JD022994

Venkatesh, J., & Kale, G. D. (2025). Ranking of CMIP6 GCMs and formulation of multi-model ensembles for precipitation projection under SSP245 and SSP585 scenarios over the Ujjani Dam catchment in India by using machine learning and conventional methods. *Environmental Science Pollution Research*, *32*, 20574–20599. https://doi.org/10.1007/s11356-025-36853-y.

Zamani, R., & Berndtsson, R. (2019). Evaluation of CMIP5 models for west and southwest Iran using TOPSIS-based method. *Theoretical and Applied Climatology*, *137*, 533–543. https://doi.org/10.1007/s00704-018-2616-0

Zhang, Y., You, Q., Ullah, S., Chen, C., Shen, L., & Liu, Z. (2023). Substantial increase in abrupt shifts between drought and flood events in China based on observations and model simulations. *Science of the Total Environment*, *876*, 162822. https://doi.org/10.1016/j.scitotenv.2023.162822